UNRAVELING THE MAGNETIC HISTORY OF PEAK RING GRANITOID ROCKS FROM THE CHICXULUB IMPACT STRUCTURE. C. M. Verhagen[1], S. M. Tikoo[1,2], J. Gattacceca[3], M. Schmieder[4], P. Rochette[3], D.A. Kring[4]. [1]Department of Earth and Planetary Sciences, Rutgers University, Piscataway Township, NJ 08854 USA; christina.verhagen@rutgers.edu, [2]Department of Geophysics, Stanford University, Stanford, CA 94305 USA, [3]Aix-Marseille Univ, CNRS, IRD, INRAE, CEREGE, Aix-en-Provence, France, [4]Lunar and Planetary Institute, Universities Space Research Association, 3600 Bay Area Boulevard, Houston, TX 77058 USA.

Introduction: Peak rings of large, complex impact craters consist of uplifted target rock and impactites emplaced during crater modification [1]. In 2016, International Ocean Discovery Program/International Continental Scientific Drilling Program (IODP/ICDP) Expedition 364 recovered peak ring samples from the Chicxulub impact structure, Yucatán Peninsula, Mexico. The pristine drillcore, M0077A, includes uplifted target rock capped with impact melt rock, suevite and post-impact Paleogene carbonate rocks. Target rock, recovered from 747.02-1334.15 meters below sea floor, (mbsf) is composed of syenogranites that are crosscut by preimpact felsic and mafic dikes as well as impact-related material [2,3]. The target granitoids, originally part of the Maya Block, crystallized 326 ± 5 million years ago (Ma) during the convergence of Gondwana and Laurentia in the formation of supercontinent Pangea [3]. Preimpact dikes likely formed concomitant to granitoid emplacement or shortly after. During the 66 Ma Chicxulub impact event, the granitoid rocks were pervasively affected by the passage of the initial impact shock wave up to ~20 GPa [4]. They were subsequently uplifted from ~10 km and emplaced during the dynamic collapse of the central uplift, forming the peak ring [5]. The initial shock alteration of the granitoids increased porosity, facilitating the circulation of post impact hydrothermal fluids driven by long-lived heat sources such as the impact melt sheet and central uplift [4, 6]. As a result, the entire sequence in M0077A shows evidence of pervasive post-impact hydrothermal activity including hydrothermal minerals such as dachiardite-Na, zeolites and hydrothermal garnet [7,8].

We use paleomagnetism to explore the magnetic history recorded within the target granitoid sequence. We employ rock magnetism and petrographic microscopy to identify the occurrence of magnetic minerals. Our efforts seek to elucidate syn- and post-impact cratering processes including shock, heating, and hydrothermal alteration and aim to identify relationships between primary and secondary magnetic components within all lithologies of the lower peak ring.

Materials and Methods:

Paleomagnetism and rock magnetism: Using a superconducting magnetometer, we measured natural remanent magnetization and conducted alternating field (AF) demagnetization experiments up to peak fields of 85 mT for 248 samples representing granitoids, preimpact mafic (dolerite) dikes and impact-related material (impact melt rocks and suevite). Origin-trending characteristic remanent magnetizations (ChRMs) were analyzed using principal component analysis to obtain magnetization directions [9]. Declination values for the drillcore were corrected using the protocol by [2]. A subset of these samples was subjected to additional rock magnetic measurements including magnetic susceptibility, hysteresis loops and Curie temperature determinations.

Petrographic microscopy: We used scanning electron microscopy (SEM) coupled with energy dispersive x-ray spectroscopy (EDS) to investigate the occurrence of magnetic minerals. Back-scatter electron (BSE) images were collected on a Hitachi S-3400N and qualitative elemental analysis and x-ray mapping were produced by a Bruker AXS Xflash X-ray detector A silicon drift detector.

Results:

Paleomagnetism and rock magnetism: Our AF demagnetization experiments yield the following ChRMs shown in **Table 1.**

Samples	Mean declination, inclination
Unbaked granitoids	219.7°, 7.4° α_{95}= 8.1 κ = 3.5 n = 120
Dolerites	236.5°, 3.7° α_{95} = 51.3 κ = 2.1 n = 8
Impact related material	174.7°, -41.5° α_{95}= 12.5 κ = 6.2 n = 26

Table 1: Mean declination and inclination values from AF demagnetization experiments. α_{95} is a confidence interval around the mean direction, κ is a precision parameter, and n is the number of samples in each fit.

For granitoid samples near dikes or impact related materials, a distance of 3.5 times the half-width of the crosscutting body was used to identify the range within granitoids that would have been fully (>580°C, the Curie temperature of magnetite) or partially (>200°C) remagnetized from dike-related heating, based on conductive cooling calculations [10]. Many granitoids within baked regions contain magnetic components that reflect the magnetic component of the nearby dike. However, some granitoids (in particular between ~900-960 mbsf) that would likely have been baked by a nearby dolerite dike at 939.08 mbsf (magnetization declination: 191.8° and inclination: 20.1°) instead

contain magnetizations with inclinations shifted towards negative inclinations (declination: 204.5°, mean inclination: -23.3°, α_{95}=14.6, κ=3.6, n=37) (**Fig. 1**).

Rock magnetic results show impact related material as well as dolerite dike samples have higher susceptibilities (average: 9.4 x 10^{-6} ± 3.9 x 10^{-6} m^3/kg, m=9.3 x 10^{-6} m^3/kg) than granitoids (average: 1.6 x 10^{-6} ± 1.1 x 10^{-6} m^3/kg, m=1.4 x 10^{-6} m^3/kg). Some granitoid samples in close proximity to dolerite dikes (~900-960 mbsf) as well as near impact related intrusions demonstrate far lower susceptibilities compared to non-baked granitoids (**Fig. 1**).

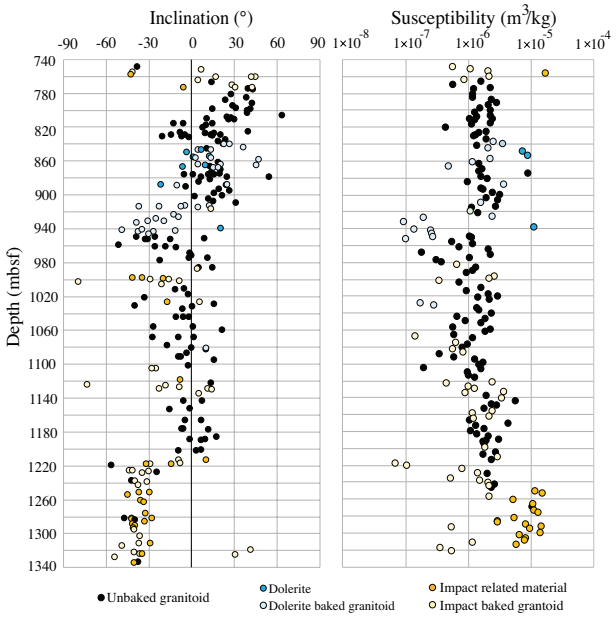

Figure 1: Inclination values from AF demagnetization and susceptibility values for all samples. Sample types are denoted as described in figure.

Petrographic microscopy: Petrographic analysis of a granitoid sample at 1216.97 mbsf (sampled near an impact related intrusion), shows Fe-oxides deposited along a fracture (**Fig. 2a**). In a dolerite sample, 939.08 mbsf, submicron Fe-oxides are visible in a clay-altered area nearby a large Fe-oxide and sulfide (**Fig. 2b**).

Discussion: The similarity of magnetization directions in dolerite and non-baked granitoid samples imply the preimpact dikes formed shortly after granite emplacement (**Table 1, Fig. 1**). The sequence above ~1220 mbsf likely moved as a cohesive block during peak ring formation [11]. Our results show the majority of non-baked granitoids contain inclinations grouped between -20 to 20°, possibly retaining their primary magnetizations as they were emplaced. However, baked granitoids near a major preimpact dolerite dike (939.08 mbsf) exhibit ChRMs with inclinations that are similar to the paleoinclination at the time of impact (~-44°) [12], suggesting they may have been remagnetized post-impact. (Fig. 1). These granitoids as well as others near major pre-impact and impact related dikes also demonstrate low susceptibilities (**Fig. 1**). Susceptibility is known to be decreased in hydrothermally altered granites [13]. Therefore, low susceptibilities, negative and steep inclination directions and petrographic evidence of secondary Fe-oxides indicate that these samples may have been magnetized by the precipitation of hydrothermal magnetic minerals post-impact. Dike contacts may have acted as important conduits for transporting hydrothermal fluids within the peak ring.

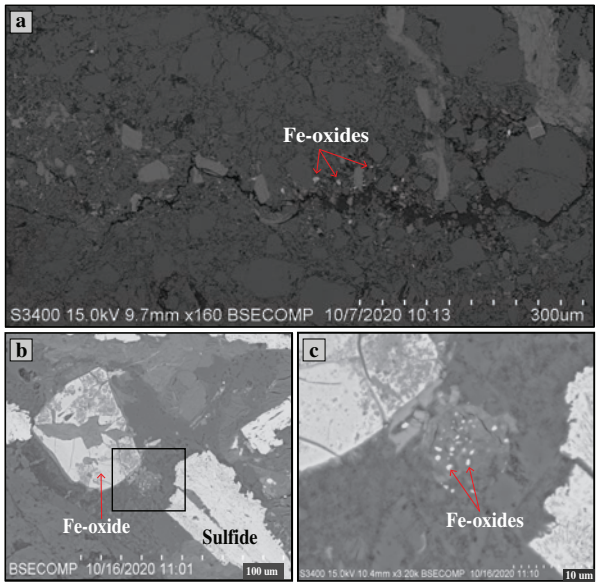

Figure 2: BSE image of a) granitoid sample 1216.97 mbsf and b,c) dolerite sample 939.08. Black square outline in b) shows the enlarged area in image c).

Acknowledgments: We thank S. Brachfeld and L. Wu for use of the SEM/EDS at Montclair State University and P. Burger for assistance with sample preparation. C. Verhagen was supported by a NSF Graduate Fellowship.

References: [1] Gulick, S. et al., (2019) *Proc. Natl. Acad. Sci, 116(39).* [2] Gulick, S. et al., (2017) *Proc. Int. Ocean Disc. Prog, 364.* [3] Zhao, J. et al., (2020) *Gondw Res. 82.* [4] Rae, A. et al., (2017) *LPS XLVIII,* Abstract #1934. [5] Morgan, J. et al., (2016) *Science 354, (6314).* [6] Abramov, O. & Kring, D. (2007) Meteorit, Planet Sci., *42(1).* [7] Kring, D. et al., (2020) *Sci. Adv., 6(eaaz3053).* [8] Simpson, S. et al., (2020) *Earth Planet. Sci. Lett. 547.* [9] Kirschvink, J. (1980) *Geophys. J. Roy. Astr. S., 62.* [10] Jaeger, J. C. (1964) *Rev. Geophys., 2(3).* [11] Riller, U. et al., (2018) *Nature, 562(7728).* [12] Urrutia-Fucugauchi, J. (2004) *Meteorit. Planet Sci., 39(6).* [13] Nédélec, A. et al., (2015) *Lithos, 212-215.*